Shear-Thinning Rheology and Geometric Asymmetry Govern Droplet Dynamics in Branched Microchannels

Rakesh Kumar,[a] Rajaram Lakkaraju,[b] and Arnab Atta*[a,c]
[a] Advanced Technology Development Centre, Indian Institute of Technology Kharagpur, Kharagpur, West Bengal 721302, India
[b] TuRbulent Interfaces And Dispersion (TRIAD) Group, Department of Mechanical Engineering, Indian Institute of Technology Kharagpur, Kharagpur, West Bengal 721302, India
[a,c] Multiscale Computational Fluid Dynamics (mCFD) Laboratory, Department of Chemical Engineering, Indian Institute of Technology Kharagpur, Kharagpur, West Bengal 721302, India

Numerical validation

Prior to the validation study, a comprehensive grid sensitivity analysis was conducted to ensure mesh-independent results. A numerical investigation was performed to explore the droplet breakup mechanism and flow regimes in a system where soybean oil acts as the dispersed phase and a shear-thinning xanthan gum solution serves as the continuous phase, following the fluid properties reported in Chiarello *et al.*[1]. The simulation captures the droplet formation dynamics under these conditions, and the results are illustrated in Figure 1, demonstrating distinct breakup regimes that align well with those typically observed in Newtonian systems.

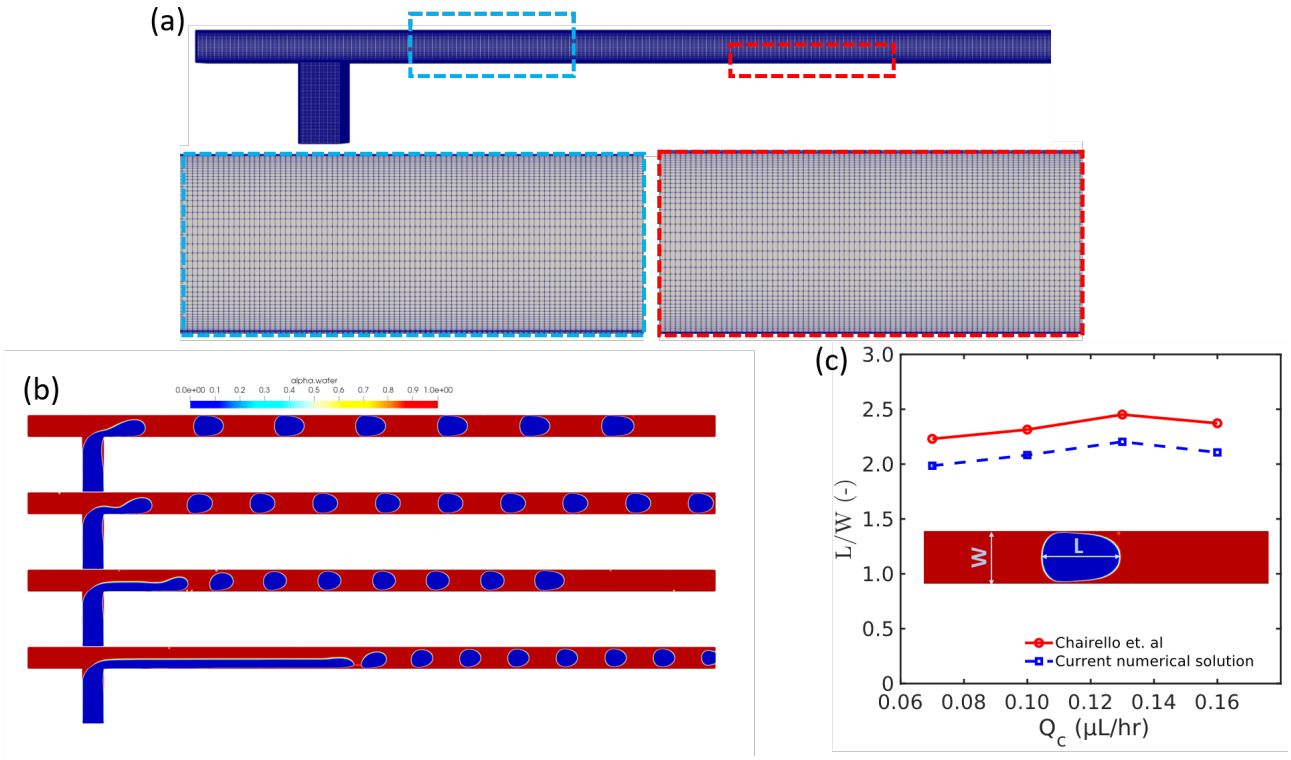

Figure 1: Comparison of the present numerical results with the experimental findings of Chiarello *et al.*[1], involving soybean oil as the dispersed phase and an aqueous xanthan gum solution as the continuous phase in a simple T-junction geometry. (a) Computational grid structure used for droplet generation, with insets highlighting the mesh refinement near the domain interior and channel walls; (b) Droplet formation at varying flow rates; and (c) Comparison between the experimental data from Chiarello *et al.*[1] and the current numerical results.

Subsequently, for a single-droplet system, the droplet length-to-channel width ratio ($\frac{L}{W}$) was

calculated across different continuous phase flow rates (Q_C) and plotted in Figure 1. The results exhibit a trend consistent with previously reported literature, with a maximum deviation of 11%.

Fabrication of microdevices

The fabrication of the branched parallel microdevices was carried out using PDMS (Polydimethylsiloxane, Sylgard 184, Dow Corning) through conventional soft lithography techniques, following photolithographic patterning and replica molding procedures [1,2], all performed within a Clean Room environment. A silicon wafer was spin-coated with SU-8 photoresist (SU-8 2050, MicroChem Corp.) and patterned using ultraviolet photolithography via a high-resolution photomask (4000 DPI) to create the master mold featuring the desired T-junction geometry. Both branches of the T-junction were designed with identical rectangular cross-sections, having a width W = 100 µm and a depth D = 77 µm. PDMS was poured over the SU-8 master to produce multiple microchannel replicas (refer to Fig. 1 (D2) in the manuscript). Each PDMS replica was irreversibly bonded to a microscope glass slide using oxygen plasma activation [3].

To render the channel surfaces hydrophilic, a surface functionalization step was performed immediately after bonding. A 5% (w/w) aqueous solution of Polyvinylpyrrolidone (PVP K90, Sigma Aldrich) was introduced into the channels at a controlled flow rate of approximately 1 µL/min using a syringe pump for 30 minutes. This was followed by rinsing with deionized water and drying with compressed air [4]. The treatment resulted in the formation of a thin hydrophilic coating on both PDMS and glass surfaces, enabling stable operation with either aqueous or oil-based continuous phases, free from wettability-related complications.

Surface modification techniques

By default, freshly fabricated PDMS microchannels exhibit hydrophobic surface characteristics, which makes them well-suited for producing aqueous droplets in Newtonian systems where oil serves as the continuous phase and water as the dispersed phase. However, implementing the reverse configuration—using water as the continuous phase and oil as the dispersed phase—poses significant challenges due to unfavorable interfacial interactions. The selection of which fluid becomes the continuous or dispersed phase is intrinsically governed by the surface wettability of the microchannel. Therefore, to facilitate the use of water as the continuous phase, surface modification of the PDMS replica is essential. In this process, the thermally cured PDMS is first subjected to oxygen plasma treatment to activate its surface, followed by immersion in a 5% (w/w) aqueous solution of Polyvinylpyrrolidone (PVP K90, Sigma Aldrich) for 30–45 minutes. This treatment allows a uniform hydrophilic PVP coating to form on the inner channel walls. The overall steps involved in the surface modification procedure are summarized in Figure 2.

The preparation of the PVP solution was carried out following the procedure recommended by Chiarello *et al.*[1], with the composition details summarized in Table 1. Surface morphology

Table 1: Experimental conditions for formulating PVP solution.

Parameters	**Parametric values**
PVP 5 wt%	0.5263 gm
DI water	10 ml
Stirring speed	800 rpm
Stirring time	2 hours under agitation
Stirring temperature	25 °C

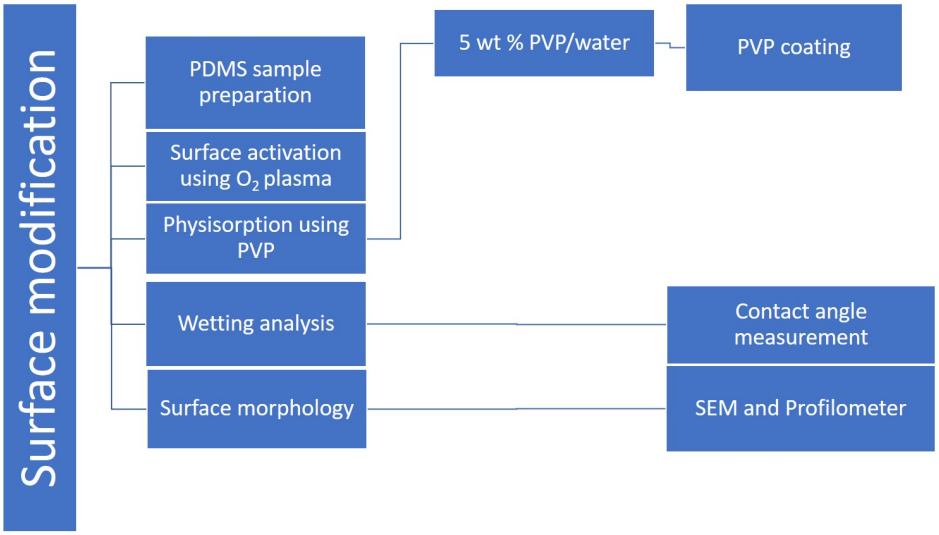

Figure 2: Process flow diagram for modifying pristine PDMS surface.

characterization was performed using a profilometer, as illustrated in Figure 3. While oxygen plasma treatment is widely employed for PDMS surface activation, its precise impact on the surface chemistry remains an area of ongoing investigation. The prevailing understanding is that oxygen plasma induces the formation of a thin, brittle "silica-like" layer, or SiO_X, on the PDMS surface[2,3].

For the coating process, a 5% (w/w) PVP/water solution was prepared by weighing 0.5623 g of Polyvinylpyrrolidone K90 (Sigma Aldrich) and dissolving it in 10 mL of deionized water. The mixture was agitated at 800 rpm for 2 hours to ensure homogeneous dispersion and to prevent adherence of the polymer to the bottom of the beaker. The entire solution preparation was conducted at room temperature (25°). The resulting solution was used directly for coating the plasma-treated PDMS surfaces, as described previously.

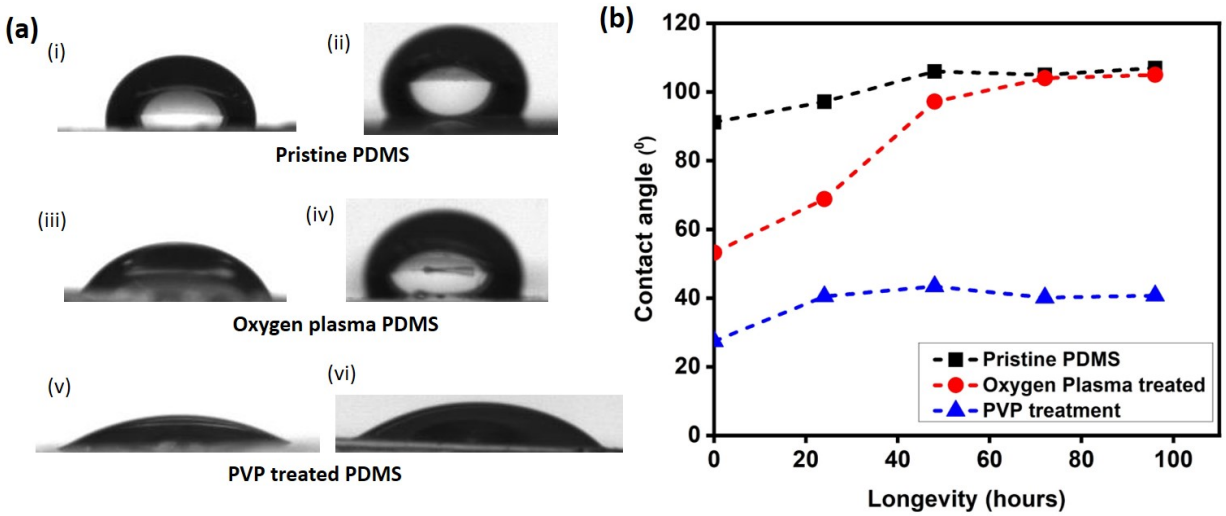

Figure 3: Average contact angle measurements for different PDMS samples as a function of aging time: (i) Pristine PDMS at day 0, (ii) Pristine PDMS at day 4, (iii) Oxygen plasma-treated PDMS at day 0, (iv) Oxygen plasma-treated PDMS at day 4, (v) PVP-treated PDMS at day 0, and (vi) PVP-treated PDMS at day 4. (b) Variation of contact angle with aging time for each treatment.

To support the above claim, Figure 3(a) illustrates the droplet shape observed on vari-

ous categories of PDMS surfaces. Qualitatively, the images confirm that PVP-treated PDMS exhibits hydrophilic characteristics after coating. This observation is further supported quantitatively in Figure 3(b). Additionally, surface morphology of the PVP-coated PDMS was examined using a surface profilometer (Dektak), revealing a coating thickness of approximately 1.5 µm, as shown in Figure 4.

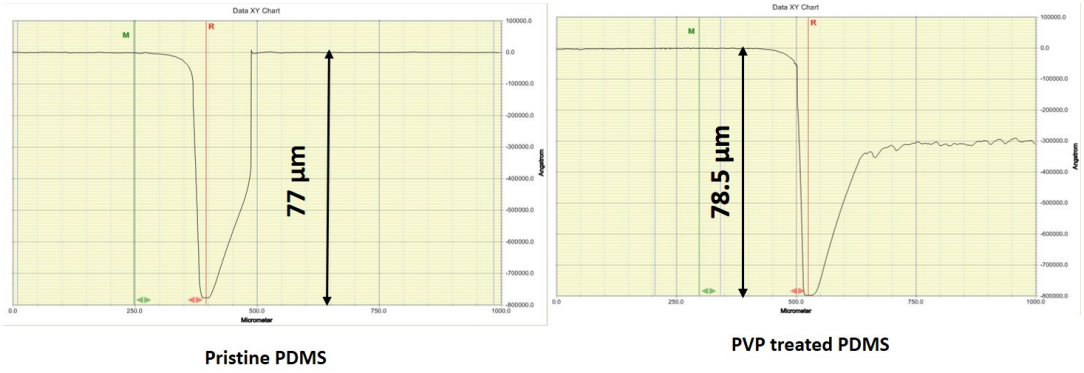

Figure 4: Profilometer images showing the surface depth of microchannels: pristine PDMS (left) and PVP-treated PDMS (right).

Shear thinning liquid preparation

Motivated by the need to use a shear-thinning continuous phase in our system, Xanthan gum (XG, $M_W = 2.7 \times 10^6$ g/mol, Sigma Aldrich) was selected to prepare the fluid. Various XG concentrations were adopted as per Chiarello *et al.*[1]. Low concentrations were specifically chosen (below 1000 ppm), since they exhibit predominantly shear-thinning behavior with minimal elastic effects[4]. At these concentrations, the first normal stress difference is negligible, ensuring Newtonian-like elastic response.

XG powder was mixed with deionized water at 1000 rpm for 24 hours to ensure uniform dispersion, followed by overnight rest to allow complete solubilization. To enhance wall wetting, a surfactant (Triton X-100, Sigma Aldrich) was added to the aqueous solution. The detailed composition of the continuous phase is summarized in Table 2[1].

Table 2: Parameters of the liquids of the non-Newtonian systems. All quantities refer to a temperature T = 25°C. The concentrations are expressed in terms of weight/weight ratio[1].

ID	XG solution	Triton X-100	stirring speed	stirring time
XG400	Xanthan gum 400 ppm	0.2 %	1000 rpm	24 hours
XG800	Xanthan gum 800 ppm	0.2 %	1000 rpm	24 hours
XG1500	Xanthan gum 1500 ppm	0.7 %	1000 rpm	24 hours

The physical properties of the solution was measured at room temperature and were summarised in Table 3. The rheology of the XG solution was characterized using a cone and plate rheometer (Anton Paar MCR 302) and measured rheological data are shown in Figure 5.

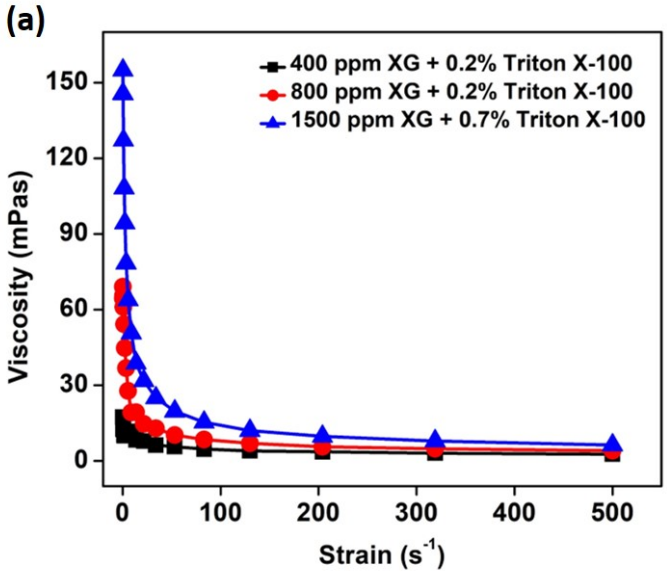

Figure 5: Rheological analysis of xanthan solutions as a function of shear rate for various xanthan concentrations in water.

Table 3: Flow consistency index and power law index after fitting to power-law model.

ID	**K**$(mPas^n)$	**n**
XG400	31.8	0.562
XG800	76.8	0.480
XG1500	304.5	0.402

Following fluid preparation and subsequent rheological analysis, the composition and rheological parameters of the fluids are summarized in Table 4.

Table 4: Physical properties of fluid

Experiments	**Fluid**		**Viscosity**	**Density**		**Interfacial Tension** (mN/m)	**Flow Consistency Index (K)**	**Shear-Thinning Parameter (n)**
	Continuous Phase	**Dispersed Phase**	μ_d $(mPas)$	ρ_c (kg/m^3)	ρ_d (kg/m^3)			
I	400-ppm xanthan gum solution + 0.2% Triton X-100	Soybean oil	49.1	990	920	3.32	31.8	0.562
II	800-ppm xanthan gum solution + 0.2% Triton X-100	Soybean oil	49.1	990	920	2.95	76.8	0.480
III	1500-ppm xanthan gum solution + 0.7% Triton X-100	Soybean oil	49.1	990	920	2.31	304.5	0.402

References

[1] E. Chiarello, A. Gupta, G. Mistura, M. Sbragaglia and M. Pierno, *Phys. Rev. Fluids*, 2017, **2**, 123602.

[2] H. Hillborg, J. Ankner, U. W. Gedde, G. Smith, H. Yasuda and K. Wikström, *Polymer*, 2000, **41**, 6851–6863.

[3] D. C. Duffy, J. C. McDonald, O. J. Schueller and G. M. Whitesides, *Anal. Chem.*, 1998, **70**, 4974–4984.

[4] X. Shen and P. E. Arratia, *Phys. Rev. Lett.*, 2011, **106**, 208101.